



0038–1098(95)00605-2

INDIRECT TUNNELING IN METAL–INSULATOR–METAL JUNCTIONS

V. Fleurov, M. Karpovski, M. Molotskii and A. Palevski

School of Physics and Astronomy, Beverly and Raymond Sackler Faculty of Exact Sciences,
Tel Aviv University, Tel Aviv 69978, Israel

A. Gladkikh

Department of Electronic Devices and Materials, Faculty of Engineering, Tel Aviv University, Tel Aviv 69978,
Israel

and

R. Kris

Graduate School of Applied Physics and Technology, Hebrew University, Jerusalem 91904, Israel

(Received 10 June 1996 by S. Alexander)

I–V characteristics of realistic MIM junctions were calculated assuming a two step indirect tunneling as the major mechanism. Electron–phonon broadening of the energy level of the intermediate defect states is taken into account. The theory is compared with our experimental investigations of Pd–MgO–Pd junctions and good quantitative agreement is achieved. The intermediate states are provided by the *F*-centers of the MgO vacancies. A consistency between the experimental data and the theory is obtained for the values of the physical parameters known from independent studies on MgO.

Keywords: A. heterojunctions, C. point defects, D. tunneling, D. electronic transport.

1. INTRODUCTION

THE PRINCIPAL mechanism of electronic transport through thin dielectric barriers is quantum mechanical tunneling. The simple theories of direct tunneling disregard imperfections within the barrier. Therefore, the electron tunnels directly from one electrode to the other across the entire dielectric layer [1]. However, real dielectrics in the metal–insulator–metal (MIM) junctions contain various defects which may assist tunneling. Tunneling via the intermediate states of the defects is usually called indirect tunneling. The relative contributions of the direct and indirect tunnelings are sensitive to the height and width of the barrier as well as to the type and concentration of the defects. The indirect contribution becomes dominant for very high and/or wide barriers [2].

Attempts to describe the tunneling in realistic junctions within the framework of direct tunneling lead to unrealistic fitting parameters [3]. At some extreme cases, the electron effective mass an order of

magnitude smaller than its bulk value is assumed, in other cases a height of the barrier 3–4 times smaller than estimated from the work function values is required. Simultaneously the barrier width and the effective tunneling area of the junction are assumed to be significantly smaller than follows from the capacitance measurements. Moreover, the observed temperature dependences of the tunneling current in realistic junctions cannot be explained by direct tunneling.

Inability of the direct tunneling model to describe the realistic systems motivates a study of indirect tunneling. Recently there have been a number of publications (e.g. [4–7] and references therein) where basic equations for the current–voltage (*I–V*) characteristics were derived and attempts to describe qualitatively the experimental results were made. However, expressions allowing for a quantitative analysis of the experimental data are still to be derived.

In this paper, we aim to derive a quantitative theory of the indirect tunneling through realistic dielectrics and to compare it with our experimental data. Our model assumes that the tunneling through the barrier is a two step process where the intermediate states are provided by defects within the dielectric layer. The main point of the model is that the intermediate defect states are broadened by a strong electron-phonon interaction. The theory employs physical microscopic parameters most of which are known from independent measurements. The expression for the I - V curve obtained in this paper fits very well our measurements for Pd-MgO-Pd junctions and allows us to determine three parameters, namely, defect density, electron localization radius and half-width of the polaron band. The values obtained for these parameters agree quite reasonably with results of other experiments and calculations.

2. CURRENT-VOLTAGE CHARACTERISTICS OF MIM TUNNELING JUNCTION

As is shown in reference [5], the current flowing via a single trap in the dielectric layer is given by

$$J = \frac{1}{e} \int g(E) [f_l(E) - f_r(E + eV)] dE, \quad (1)$$

where V is the voltage across the junction, $f_l(E)$ and $f_r(E)$ are the Fermi distribution functions in the left and the right electrodes, and e is the electron charge. The conductance, $g(E)$, depends on the widths Γ_l and Γ_r , determined by the corresponding tunneling amplitudes. The latter are assumed to be very small as compared to the electron energy E_0 in the defect ($\Gamma_{l,r} \ll E_0$), which allows one to express the conductance as

$$g(E) = \frac{4e^2}{\pi\hbar} \frac{\Gamma_l(E)\Gamma_r(E)}{\Gamma_l(E) + \Gamma_r(E)} \delta(E - E_0). \quad (2)$$

The popular insulators employed in the MIM junctions are ionic dielectric crystals, where electrons interact strongly with longitudinal optical phonons. It was shown references [4 and 6] that such an interaction may give a strong impact on the I - V characteristics. In the crystals with strong electron-phonon interaction, the probability of the elastic indirect tunneling is negligible compared to multiphonon processes. The electron energy in the defect, E_0 , is broadened to a polaron band [6] and therefore the δ function in equation (2) should be substituted by

$$W(E) = \frac{1}{\sqrt{2\pi\sigma^2}} \exp \left\{ -\frac{(E - E_0)^2}{2\sigma^2} \right\}, \quad (3)$$

where σ is the half-width of the polaron band. Similar

equations are widely used for interpretation of experiments on tunneling electron transport in chemical and biological systems [8].

The current density j is the sum of the contributions (1) coming from all the defects in a unit area

$$j = \frac{4e}{\hbar} \int_0^a dz n_v(z) \int_0^\infty dE \frac{\Gamma_l(E, V, z)\Gamma_r(E, V, z)}{\Gamma_l(E, V, z) + \Gamma_r(E, V, z)} \times W(E, V, z) [f_l(E) - f_r(E + eV)]. \quad (4)$$

Here, $n_v(z)$ is the average defect density at distance z from the edge of the left electrode, a is the thickness of the dielectric layer. Equation (4) is valid only for low defect densities ($n_v^{1/3}a \ll 1$) when the contributions of tunneling via more than one defect state can be neglected.

In order to calculate $\Gamma_{l,r}(E)$, the standard approximations as in the theory of the direct tunneling [1] are used. The electron energies in our further calculations will be counted from the bottom of the conduction band of the left electrode metal. The behavior of the metal electron tunneling inside the dielectric is described by the wave function

$$\psi_c(\rho, z) = \frac{2}{\sqrt{\Omega}} \frac{k_\perp}{k_\perp + i\kappa(m_c/m_e)} e^{ik_\parallel\rho - \kappa(s+z)}, \quad z \geq 0, \quad (5)$$

where

$$\kappa = \sqrt{\frac{2m_e}{\hbar^2} \left(U_0 - \frac{\hbar^2 k_\perp^2}{2m_e} \right)},$$

U_0 is the barrier height, k_\perp and k_\parallel are the components of the electron wave vector perpendicular and parallel to the interface, Ω is the volume of the metal. The reference point for the coordinate z is chosen to be at the defect, which is situated at a distance s from the interface.

It is expected that the principal contribution to the indirect tunneling will come from the F -centres. MgO is known [9] to contain a large amount of the anion vacancies, which capture two electrons in the ground state creating F -centers. F^+ -centers (vacancies with only one electron captured) have smaller localization radii [10] and their contribution is less important. Therefore, we believe that the two steps of the indirect tunneling are as follows. First, one of the two electrons of the F -center tunnels to the corresponding electrode, and then an electron from the other electrode arrives at the vacant place in the F -center. As a result we have to consider the behavior of the electron in the Coulomb field

$$U_C(\rho, z) = -\frac{e^2}{\epsilon_0 \sqrt{\rho^2 + z^2}}, \quad (6)$$

where ϵ_0 is the static dielectric permeability. Such a potential has been calculated in detail [11, 12]. At a large distance from the defect the effective mass approximation yields the electron wave function in the form

$$\psi_0(\rho, z) = \frac{1}{\sqrt{\pi R^3}} \exp\left(-\frac{1}{R} \sqrt{\rho^2 + z^2}\right), \quad (7)$$

where R is the electron localization radius.

The transition matrix element between the defect (7) and metal (5) states in the field of the defect (6) reads

$$\begin{aligned} \langle c|U_C|0\rangle = & -4\sqrt{\frac{\pi}{\Omega R^3}} \frac{e_0^2}{\epsilon_0 \kappa_0} \frac{k_\perp}{k_\perp + i\kappa(m_c/m_e)} \\ & \times \left(\frac{1}{\kappa - \kappa_0} e^{-\kappa_0 s} - \frac{2\kappa_0}{\kappa^2 - \kappa_0^2} e^{-\kappa s} \right), \end{aligned} \quad (8)$$

where

$$\kappa_0 = \sqrt{k_\parallel^2 + (1/R^2)}.$$

The width of the localized level caused by the tunneling of electrons to the metal states whose density is

$$d\rho_f = \frac{\Omega k_\parallel dk_\parallel dk_\perp}{4\pi^2 dE} \quad (9)$$

can be obtained by means of the Fermi golden rule

$$\begin{aligned} \Gamma_l(\epsilon, z) = & \pi \int |\langle c|U_C|0\rangle|^2 d\rho_f \\ = & 8Ry^* \mathcal{F}(\zeta, \gamma, \epsilon, \mu, \eta_0). \end{aligned} \quad (10)$$

Here

$$\begin{aligned} \mathcal{F}(\zeta, \gamma, \epsilon, \mu, \eta_0) = & \mu^{3/2} \epsilon^{3/2} \eta_0^3 \int_0^1 dx \frac{x\sqrt{1-x^2}}{[\gamma(1-x^2) + \mu u(x)]v(x)} \\ & \times \left(\frac{e^{-\zeta\sqrt{v(x)}}}{\sqrt{u(x)} - \sqrt{v(x)}} - \frac{2\sqrt{v(x)} e^{-\zeta\sqrt{u(x)}}}{u(x) - v(x)} \right)^2, \end{aligned}$$

and

$$u(x) = \beta - \epsilon(1-x^2), \quad v(x) = \eta_0^2 + \epsilon\mu x^2,$$

$Ry^* = m_e e_0^4 / 2\hbar^2 \epsilon_0^2$, $E_p = \hbar^2 / 2m_e r_0^2$, r_0 is the lattice spacing in the dielectric; $\zeta = s/r_0$, $\gamma = U_0/E_p$, $\epsilon = E/E_p$, $\eta_0 = r_0/R$, and $\mu = m_c/m_e$. The tunneling width Γ_r is also given by equation (10) in which s is substituted by $a-s$.

The last expression does not account for the voltage applied across the junction. As was shown for the double barrier structures [13] the application of a strong electric field can increase Γ by several orders of magnitude. Therefore, the quantitative theory

cannot ignore this effect. It should be noted that this $\Gamma(V)$ dependence has been neglected in the previous publications [4–7].

As first suggested by Simmons [14] and successfully used in recent calculations [15, 16] the electrical field effect can be accounted for by substituting the barrier height U by its average value in the field. In our case, it means that the average barrier heights are

$$U_l = U - \frac{1}{2}eV \frac{s}{a} \quad \text{and} \quad U_r = U - \frac{1}{2}eV \left(1 + \frac{s}{a}\right)$$

for the left and right electrodes, respectively. In addition, we should account for the linear shift of the defect energy E_0 and substitute it with

$$E_0(s, V) = E_0 - eV \frac{s}{a}.$$

Therefore, the function $W(E)$ equation (3) becomes s and V dependent.

3. EXPERIMENTAL RESULTS AND DISCUSSION

Three sets of Pd–MgO–Pd (30, 40 and 50 Å) and Au–MgO–Au (40, 60 and 80 Å) junctions with different MgO thicknesses were deposited onto sapphire substrate. The standard vacuum evaporation ($p \sim 1 \times 10^{-6}$ Torr) by electron gun was employed in consecutive deposition of the layers. The top electrode layer was evaporated through the mesh with an area of $100 \times 100 \mu\text{m}$. Two terminal I – V characteristics of the junctions were measured at room temperature using HP-4145B parameter analyzer. The results of the electrical measurement for Pd–MgO–Pd junctions are presented in Fig. 1 and discussed below.

The theory developed in Section 2 is now applied to a realistic Pd–MgO–Pd structure. The barrier height counted from the bottom of the metal conduction band at the Pd–MgO interface is obtained as $U_0 = E_f + \Phi - \chi = 11.12$ eV where $E_f = 7$ eV [17] is the metal Fermi energy, $\Phi = 5.12$ eV [18] is the metal work function, and $\chi = 1$ eV [19] is the affinity of the dielectric. The following parameters are employed $m_c = 2.1m_0$ [17], $m_e = 0.35m_0$ [20], $r_0 = 2.105$ Å, $\epsilon_0 = 9.8$.

The electron tunnels via a nonrelaxed defect state [6] which can be also revealed, e.g. in luminescence spectra. Arguments in favor of an active participation of the F -centers in tunneling via MgO layers were presented above. The level positions of the centers can be obtained from previous experiments [12]. The luminescence band with a maximum at 2.3 eV is caused by the

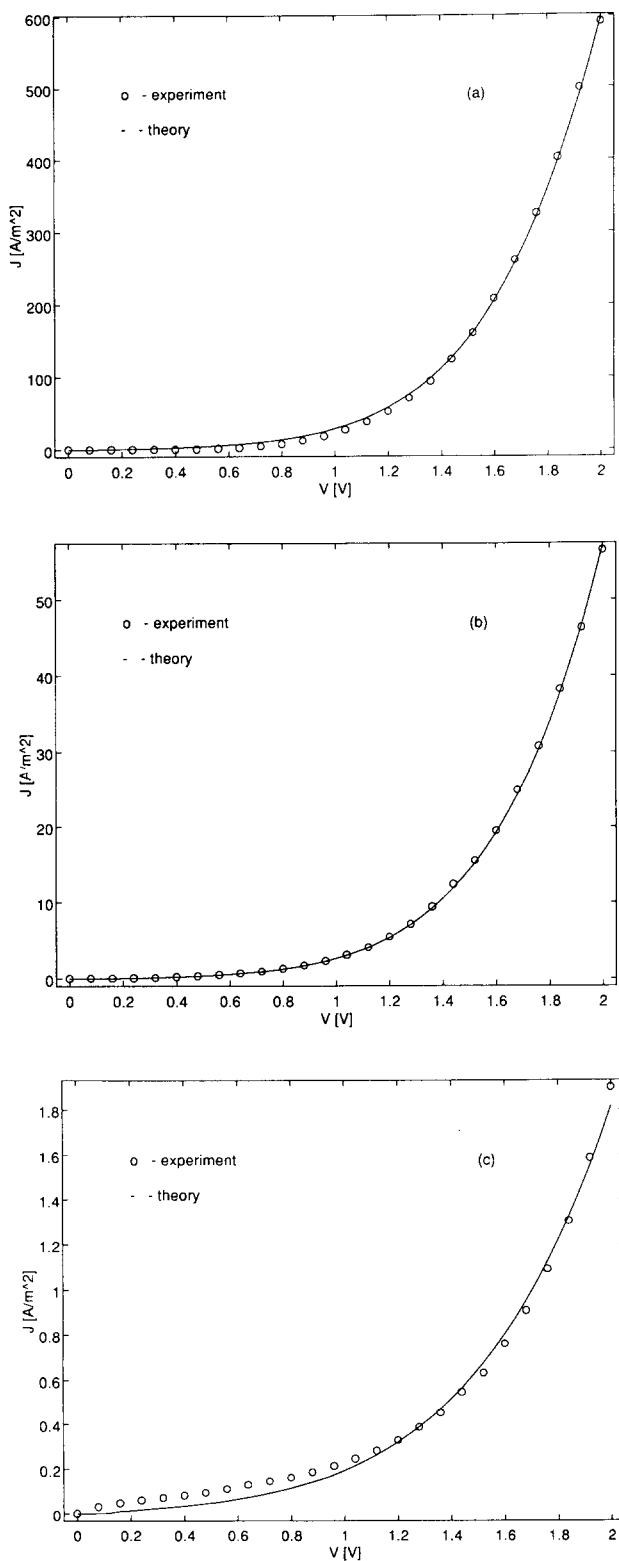


Fig. 1. I - V characteristics of the MIM junctions for 30 Å (a), 40 Å (b), and 50 Å (c) dielectric layers. Circles denote the experimental data for the Pd-MgO-Pd junctions. Solid lines are theoretical curves.

${}^1T_{1u} \rightarrow {}^1A_{1g}$ transitions. Since the excited ${}^1T_{1u}$ state is known [21] to lie 0.06 eV below the bottom of the MgO conduction band, the nonrelaxed ${}^1A_{1g}$ states which contribute to the indirect tunneling, lay at 2.36 eV below the conduction band. Accounting for the above value U_0 this level lies at $E_0 = 8.76$ eV above the bottom of the metal conduction band.

Figure 1 shows that at $R = 3.63 \text{ \AA}$ and $\sigma = 0.47\text{--}0.57 \text{ eV}$ the theoretical current-voltage dependences agree well with the experiment. The density of the tunneling centers (F -centers) corresponds to the observed current density and varies in a narrow interval from $n_v = 1.3 \times 10^{16} \text{ cm}^{-3}$ to $n_v = 3.1 \times 10^{16} \text{ cm}^{-3}$ for different samples. This value is quite reasonable for MgO. In many situations it may be, in principle, even larger, e.g. samples with n_v up to 10^{18} cm^{-3} were used in the luminescence measurements [12, 22]. As for the half-width σ , it may be compared with the half-width of the F -center luminescence band in MgO (0.72 eV [12], 0.65 eV [22]). A certain deviation of these results can be attributed to the fact that the two experimental situations are different since the initial electron states differ. Such large values of the level widths are caused by an extremely strong electron-phonon coupling typical of MgO. According to the calculations carried out by Wilson and Wood [21] the Huang-Rhys factor for the ${}^1T_{1u} \rightarrow A_{1g}$ transitions in the F -centers is very large $S = 14$. A reasonable value of the radius R of the nonrelaxed state is also obtained. It is to be expected that this value is larger than the radius of 1.66 Å calculated for the relaxed state [23].

Our assumption is that the parameters R and σ relate to the bulk properties of MgO; thus, changing the metallic electrodes would not effect their values. In order to check this, I - V characteristics of tunneling Au-MgO-Au junctions were measured. The parameters $R = 3.82 \text{ \AA}$ and $\sigma = 0.58 \text{ eV}$ were extracted by the procedure similar to that described above and they appeared to be very close to the corresponding values in the Pd-MgO-Pd junctions. It certainly favors their bulk character.

It is emphasized that other experimental techniques produce little information on the localization radius of a MgO F -center or any other data on the structure of the electron wave function. This sort of information for paramagnetic centers is often obtained by means of electron nuclear double resonance (see, e.g. [24]) which, however, appears to be useless in our case when dealing with nonmagnetic defect. It means that analyzing the I - V characteristics gives us a way to study the electron wave function of such centers.

4. CONCLUSIONS

To summarize we have calculated the I - V characteristics for the realistic MIM junctions assuming phonon assisted two step indirect tunneling to be the main process. Our model describes excellently the experimental observations. Most of the parameters used in the model are taken from independent measurements published elsewhere. The other three parameters, namely, the defect concentration n_d , localization radius R , and the half-width σ appear to be bulk characteristics of MgO independent of the electrodes. Their magnitudes are in reasonable agreement with theoretical estimates and data available by other experimental techniques.

REFERENCES

1. J.G. Simmons, *Handbook of Thin Film Technology* (Edited by L.I. Meisel & R. Gland). McGraw-Hill, New York (1983).
2. M. Naito & M.R. Beasley, *Phys. Rev.* **B35**, 2548 (1987).
3. K.L. Chopra, *Thin Film Phenomena*. McGraw-Hill, New York (1969).
4. A.D. Stone & P.A. Lee, *Phys. Rev. Lett.* **54**, 1196 (1987).
5. A.I. Larkin & K.A. Matveev, *Sov. Phys.-JETP* **66**, 580 (1987).
6. L.I. Glazman & R.I. Shekhter, *Sov. Phys.-JETP* **67**, 163 (1988); *Solid State Commun.* **66**, 65 (1988).
7. I.A. Devyatov & M.Yu. Kupriyanov, *JETP* **77**, 874 (1993).
8. V.I. Goldanskii, L.I. Trakhtenberg & V.N. Fleurov, *Tunneling Phenomena in Chemical Physics*. Gordon and Breach, New York (1989).
9. J. Dresner & B. Goldstein, *J. Appl. Phys.* **47**, 1038 (1976).
10. Q.S. Wang & N.A.W. Holzwarth, *Phys. Rev.* **B41**, 3211 (1990).
11. R.F. Wood & T.M. Wilson, *Phys. Rev.* **15**, 3700 (1977).
12. G.P. Summers, T.M. Wilson, B.T. Jeffries, H.T. Tohver, Y. Chen & M.M. Abraham, *Phys. Rev.* **B27**, 1283 (1983).
13. J.-P. Peng, H. Chen & S.-X. Zhou, *Phys. Rev.* **B43**, 12042 (1991).
14. J.G. Simmons, *J. Appl. Phys.* **34**, 1793 (1963).
15. V.N. Dobrovolskii, G.K. Ninidze & V.N. Petrusenko, *Semiconductors* **28**, 390 (1994).
16. J.A. Porto, J. Sanchez-Dehesa, L.A. Cury, A. Nogaret & J.C. Portal, *J. Phys.: Condens. Matter* **6**, 887 (1994).
17. O.K. Anderson & A.R. Mackintosh, *Solid State Commun.* **6**, 285 (1968).
18. R.C. Weast (ed.), *CRC Handbook of Chemistry and Physics*, 70th Edition, CRC Press Inc., Boca Raton, Florida (1989-90).
19. R.J. Stevenson & E.B. Hensley, *J. Appl. Phys.* **32**, 1661 (1961).
20. Y.-N. Xu & W.Y. Ching, *Phys. Rev.* **B27**, 4461 (1991).
21. T.M. Wilson & R.F. Wood, *J. Phys. (Paris), Colloq.* **37**, C7-190 (1976).
22. L.A. Kappers, R.L. Kroes & E.B. Hamsley, *Phys. Rev.* **B1**, 4151 (1970).
23. R. Pandley & J.M. Vail, *J. Phys.: Condens. Matter* **1**, 2801 (1989).
24. J.-M. Spaeth & F.K. Koshnick, *J. Phys. Chem. Solids* **52**, 1 (1991).